Atmos. Chem. Phys. Discuss., 13, 28973–29006, 2013
www.atmos-chem-phys-discuss.net/13/28973/2013/
doi:10.5194/acpd-13-28973-2013

Atmospheric Chemistry and Physics Discussions
Open Access

This discussion paper is/has been under review for the journal Atmospheric Chemistry and Physics (ACP). Please refer to the corresponding final paper in ACP if available.

An MCM modeling study of nitryl chloride ($ClNO_2$) impacts on oxidation, ozone production and nitrogen oxide partitioning in polluted continental outflow

T. P. Riedel[1,2], G. M. Wolfe[3,4], K. T. Danas[2], J. B. Gilman[5,6], W. C. Kuster[5,6], D. M. Bon[5,6], A. Vlasenko[7], S.-M. Li[7], E. J. Williams[5,6], B. M. Lerner[5,6], P. R. Veres[5,6], J. M. Roberts[5], J. S. Holloway[5], B. Lefer[8], S. S. Brown[5], and J. A. Thornton[2]

[1]Department of Chemistry, University of Washington, Seattle, Washington, USA
[2]Department of Atmospheric Sciences, University of Washington, Seattle, Washington, USA
[3]Joint Center for Earth Systems Technology, University of Maryland Baltimore County, Baltimore, Maryland, USA
[4]Atmospheric Chemistry and Dynamics Laboratory, NASA Goddard Space Flight Center, Greenbelt, Maryland, USA

[5]NOAA Earth System Research Laboratory, Chemical Sciences Division, Boulder, Colorado, USA
[6]Cooperative Institute for Research in Environmental Sciences, University of Colorado, Boulder, Colorado, USA
[7]Air Quality Research Division, Science and Technology Branch, Environment Canada, Canada
[8]Department of Earth and Atmospheric Sciences, University of Houston, Houston, Texas, USA

Received: 13 October 2013 – Accepted: 15 October 2013 – Published: 6 November 2013

Correspondence to: J. A. Thornton (thornton@atmos.washington.edu)

Published by Copernicus Publications on behalf of the European Geosciences Union.

Abstract

Nitryl chloride ($ClNO_2$) is produced at night by reactions of dinitrogen pentoxide (N_2O_5) on chloride containing surfaces. $ClNO_2$ is photolyzed during the morning hours after sunrise to liberate highly reactive chlorine atoms (Cl·). This chemistry takes place primarily in polluted environments where the concentrations of N_2O_5 precursors (nitrogen oxide radicals and ozone) are high, though it likely occurs in remote regions at lower intensities. Recent field measurements have illustrated the potential importance of $ClNO_2$ as a daytime Cl· source and a nighttime NO_x reservoir. However, the fate of the Cl· and the overall impact of $ClNO_2$ on regional photochemistry remain unclear. To this end, we have incorporated $ClNO_2$ production, photolysis, and subsequent Cl· reactions into an existing Master Chemical Mechanism (MCM version 3.2) box model framework using observational constraints from the CalNex 2010 field study. Cl· reactions with a set of alkenes and alcohols, and the simplified multiphase chemistry of N_2O_5, $ClNO_2$, HOCl, $ClONO_2$, and Cl_2, none of which are currently part of the MCM, have been added to the mechanism. The presence of $ClNO_2$ produces significant changes to oxidants, ozone, and nitrogen oxide partitioning, relative to model runs excluding $ClNO_2$ formation. From a nighttime maximum of 1.5 ppbv $ClNO_2$, the daytime maximum Cl· concentration reaches 1×10^5 atoms cm^{-3} at 7 a.m., reacting mostly with a large suite of volatile organic compounds (VOC) to produce 2.2 times more organic peroxy radicals in the morning than in the absence of $ClNO_2$. In the presence of several ppbv of nitrogen oxide radicals (NO_x = NO + NO_2), these perturbations lead to similar enhancements in hydrogen oxide radicals (HO_x = OH + HO_2). Neglecting contributions from HONO, the total integrated daytime radical source is 17 % larger when including $ClNO_2$, which leads to a similar enhancement in integrated ozone production of 15 %. Detectable levels (tens of pptv) of chlorine containing organic compounds are predicted to form as a result of Cl· addition to alkenes, which may be useful in identifying times of active Cl· chemistry.

1 Introduction

Chlorine atoms (Cl·) are highly reactive, often having rate constants for reactions with volatile organic compounds (VOC) that are factors of 10 to 200 larger than the hydroxyl radical, OH, which is considered the atmosphere's primary initiator of oxidation. As a result, the presence of Cl· can lead to shorter lifetimes for VOC and an enhanced radical pool which can potentially enhance the production of ozone in polluted areas. The global tropospheric Cl· budget remains uncertain, with a large range in recent studies (~ 15–40 Tg Cl yr^{-1}) developed from indirect means (Allan et al., 2007; Platt et al., 2004) as tropospheric Cl· concentrations are not presently measurable by existing methods. There are a number of potential Cl· sources in the troposphere, the major sources are outlined in Reactions (R1)–(R5).

$$HCl + OH \rightarrow Cl\cdot + H_2O \qquad (R1)$$

$$Cl_2 + h\nu \rightarrow 2Cl\cdot \qquad (R2)$$

$$BrCl + h\nu \rightarrow Cl\cdot + Br\cdot \qquad (R3)$$

$$ClNO + h\nu \rightarrow Cl\cdot + NO \qquad (R4)$$

$$ClNO_2 + h\nu \rightarrow Cl\cdot + NO_2 \qquad (R5)$$

The reaction of hydrochloric acid (HCl) with the hydroxyl radical (OH) is a daytime source of Cl·. Typical HCl mixing ratios in the troposphere vary from 100–5000 pptv with the highest found in polluted regions with direct HCl emissions from industrial processes and acid displacement of aqueous chloride by HNO_3 and H_2SO_4 (Keene et al., 2007). Cl· formed by HCl + OH tend to peak around midday with the peak in OH formed from O(^{1}D) + H_2O. Additionally, the oxidation of many VOC by Cl· proceeds via a hydrogen abstraction to form HCl, thus recycling this Cl· source.

Photolysis of molecular chlorine (Cl_2) produces two Cl· and has been the focus of many Cl· investigations since it was first measured at elevated concentrations in ambient air (Finley and Saltzman, 2006, 2008; Lawler et al., 2011; Riedel et al., 2012a; Spicer et al., 1998). Cl_2 mixing ratios were often on the order of tens of pptv with maximum reported mixing ratios near 100–200 pptv. Direct Cl_2 emissions are related to power generation, water treatment, and oil refineries (Sarwar and Bhave, 2007). Recently, a low pH Cl_2 production channel that may be atmospherically relevant has been identified in the reaction of N_2O_5 with chloride containing substrates, which involved $ClNO_2$ as an intermediate (Roberts et al., 2008). In addition, Cl_2 can be formed in situ through multiphase chemistry involving chlorine nitrate ($ClONO_2$) and hypochlorous acid (HOCl). These species, in turn, can photolyze to reform Cl· or ClO or react on acidic, chloride-containing particles to form Cl_2. In polluted air, the reaction of ClO with NO, which completes a null cycle producing Cl· and NO_2, limits the potential for multiphase Cl_2 formation.

BrCl photolysis to form Cl· and atomic bromine is also thought to be an important Cl· source, especially in remote regions. In polar regions, BrCl mixing ratios on the order of tens of pptv have been measured (Buys et al., 2013; Foster et al., 2001; Spicer et al., 2002). To our knowledge there have been no reported observations of BrCl in ambient air outside of polar regions (Finley and Saltzman, 2008). BrCl can form through heterogeneous reactions of $BrONO_2$ and HOBr on acidic, chloride-containing particles in an analogous manner to the Cl_2 formation reactions described above or through reactions of $ClONO_2$ and HOCl on acidic, bromide-containing particles.

Nitrosyl chloride (ClNO) has also been proposed as a potential Cl· source (Raff et al., 2009). These theoretical and laboratory studies have yet to be confirmed by field measurements of ClNO in ambient air. Using a regional 3-D chemical transport model, Raff et al. predict that ClNO mixing ratios in polluted marine areas could reach ppbv values. That said, the hydrolysis of ClNO at moderate and high relative humidity (RH > 20 %) will likely be sufficiently rapid to prevent the buildup of appreciable atmospheric concentrations of ClNO (Karlsson and Ljungström, 1996; Rubasinghege and Grassian, 2012; Scheer et al., 1997).

Since its proposed atmospheric formation by Finlayson-Pitts et al. (1989) and first observation in ambient air by Osthoff et al. (2008), nitryl chloride ($ClNO_2$) has been observed during a number of different field studies worldwide with nighttime maximum

mixing ratios ranging from tens of pptv to over 2 ppbv (Kercher et al., 2009; Mielke et al., 2011; Osthoff et al., 2008; Phillips et al., 2012; Riedel et al., 2012a; Thornton et al., 2010; Young et al., 2012). These observations have occurred in both continental and marine locations illustrating the importance of $ClNO_2$ as a Cl· source in a variety of different environments. $ClNO_2$ represents a Cl· source with clear anthropogenic origins as it is formed at night by reactions involving NO_x (NO_2 + NO), ozone, and chloride containing aerosols. Anthropogenic activities associated with power generation, motor vehicle use, and agriculture now dominate the global NO_x source (Jaegle et al., 2005). Natural sources of NO_x, such as microbial activity, lightning, and wildfires, are also significant globally, but the impact of these NO_x sources on $ClNO_2$ formation remain unknown. At night, a fraction of NO_x is converted into $ClNO_2$ through Reactions (R6)–(R8). The branching ratio between Reactions (R8a) and (R8b), commonly referred to as the $ClNO_2$ yield (φ_{ClNO_2}), is determined by the efficiency of $ClNO_2$ formation from heterogeneous reactions of N_2O_5. The φ_{ClNO_2} and the N_2O_5-particle reaction probability, $\gamma(N_2O_5)$, are uncertain quantities that can vary significantly depending on a number of factors such as particulate water, chloride, nitrate, and organic content (Badger et al., 2006; Bertram and Thornton, 2009; McNeill et al., 2006; Mentel et al., 1999; Thornton et al., 2003). After sunrise, the photolysis of $ClNO_2$ produces Cl· and NO_2, thereby partially circumventing the removal of NO_x through the formation and loss of $2HNO_3$ (R8a).

$$NO_2 + O_3 \rightarrow NO_3 + O_2 \tag{R6}$$

$$NO_3 + NO_2 \leftrightarrow N_2O_5 \tag{R7}$$

$$N_2O_5 + H_2O \xrightarrow{\gamma} 2HNO_3 \tag{R8a}$$

$$N_2O_5 + Cl^- \xrightarrow{\gamma} \varphi_{ClNO_2} ClNO_2 + (2 - \varphi_{ClNO_2}) NO_3^- \tag{R8b}$$

The Cl· budget, hydrogen oxide and organic peroxy radical abundance (RO_x = OH + HO_2 + RO_2), NO_x lifetime and partitioning among other forms of reactive nitrogen, and the net ozone production rate are linked through photochemical oxidation of VOC. As shown in Reactions (R9)–(R12) the oxidation of a hydrocarbon (RH) is initiated by reaction with OH or Cl· to form the organic peroxy radical (RO_2). In polluted regions, the dominant fate of RO_2 is to react with NO. The dominant channel of this reaction eventually leads to a closed shell oxygenated hydrocarbon (OVOC – oxygenated volatile organic compound), hydroperoxyl radical (HO_2) and NO_2, while the minor channel leads to an alkyl nitrate ($RONO_2$). If the RO_2 is an acyl peroxy radical, then reaction with NO_2 produces acyl peroxy nitrates (APN) such as acetyl peroxy nitrate (PAN). NO also reacts with HO_2 to form NO_2 and OH. Through these reactions ozone is produced from the photolysis of NO_2.

$$\mathrm{RH + OH \rightarrow RO_2 + H_2O} \tag{R9}$$

$$\mathrm{RH + Cl\cdot \rightarrow RO_2 + HCl} \tag{R10}$$

$$\mathrm{RO_2 + NO \rightarrow OVOC + HO_2 + NO_2} \tag{R11a}$$

$$\mathrm{RO_2 + NO \rightarrow RONO_2} \tag{R11b}$$

$$\mathrm{RO_2 + NO_2 \leftrightarrow APN} \tag{R12}$$

From the above discussion, we expect that $ClNO_2$ acts similarly, though not exactly the same, as an OH source such as that from nitrous acid (HONO) photolysis or $O(^1D)$ + H_2O. When the radical pool is terminated via cross reactions between RO_x and NO_x, a higher production rate of HO_x or Cl· will nearly linearly increase the ozone production rate (Daum et al., 2000; Kleinman, 2005). Moreover, at high NO, production of an RO_2 by Cl· attack directly increases the steady state concentration of OH and HO_2 due to the rapid cycling between OH, HO_2 and RO_2. However, the increased RO_2 due to Cl· arises from a potentially different pool of hydrocarbons than that from OH, given the large differences in RH abundance and relative reactivity towards OH and Cl·. Moreover, $ClNO_2$ photolysis predominantly occurs in the first few hours after sunrise, well before the maximum OH production rate from $O(^1D)$ + H_2O and before the maximum in NO/NO_2. Thus, the full impact of $ClNO_2$ on ozone production, VOC

lifetime and NO_x abundance and partitioning may not be the same as simply scaling the daytime average HO_x production rate.

Here we examine the effects of $ClNO_2$ formation as predicted by a detailed box model that incorporates the Master Chemical Mechanism and is constrained by ground and ship-based ambient measurements taken during the CalNex 2010 field study. The aim is not to replicate specific observations or conditions, but rather to use the model to develop conceptual insights into the effect of a morning pulse of chlorine atoms in polluted air. We use the model to assess the impact of $ClNO_2$ on the Cl· budget, RO_x abundance, NO_x lifetime and partitioning, and the net ozone production rate.

2 Measurements and model description

We chose to constrain a box model using data taken during the CalNex field study, which occurred in May and June of 2010 in the southern California region (Ryerson et al., 2013). The goal of these modeling studies is not to replicate the evolution of specific air masses in the LA Basin, but instead to more generally probe the effect of multiphase reactive nitrogen and reactive halogen chemistry on radical budgets, ozone production, and the fate of NO_x in polluted coastal regions. There were multiple measurement platforms involved in CalNex, three of which recorded both $ClNO_2$ and extensive VOC measurements: the Research Vessel *Atlantis*, a ground site located on the California Institute of Technology campus in Pasadena, CA, and aircraft measurements taken on the NOAA WP-3D. Though the R/V *Atlantis* sampled in many locations along the southern California coast, we focus on the measurements made in and around Los Angeles urban outflow due to the added constraints provided by the Pasadena ground site measurements. $ClNO_2$ mixing ratios in the nocturnal outflow from the Los Angeles region were commonly over 500 pptv with maximums on the order of 2 ppbv (Riedel et al., 2012a; Wagner et al., 2012).

Cl· chemistry was incorporated into an existing model framework described in Wolfe and Thornton (2011) which is based on the Master Chemical Mechanism version 3.2 (MCM) developed at the University of Leeds (more information available at http://mcm.leeds.ac.uk/MCM) (Bloss et al., 2005; Jenkin et al., 1997, 2003; Saunders et al., 2003). Use of the MCM allows for explicit tracking of approximately 2800 chemical species and about 9000 different reactions with reaction rate constants derived from the International Union of Pure and Applied Chemistry (IUPAC) kinetics database (http://www.iupac-kinetic.ch.cam.ac.uk).

In total, 44 of the VOC measured at the Pasadena site are used to constrain the model. However, certain VOC, such as ethanol (median value = 8.2 ppbv) and acetone (median value = 3.8 ppbv), measured at the Pasadena ground site appeared to often be dominated by highly localized emissions. To more generally represent an urban air mass in the model, ground site VOC measurements were scaled by those measured on the R/V *Atlantis*. A smaller number of VOC were measured aboard the R/V *Atlantis*, so species not represented in the R/V *Atlantis* dataset were scaled by species of similar structure (i.e., similar functional groups). For example, methanol was measured with median levels of approximately 6 ppbv and 1 ppbv at the ground site and on the ship, respectively. Ethanol, however, was only measured at the ground site. To estimate ethanol levels in the urban outflow and be more representative of what the R/V *Atlantis* might have sampled, the ground site ethanol mixing ratios were simply scaled down by 1/6. For a complete list of the measured VOC used in the model see Supplement Table T-1.

VOC and HCl mixing ratios are held to their ship-scaled hourly average diurnal profiles for a 69 h "spin-up" period. The diurnal HCl profile used is shown in Fig. S1. NO_2, O_3, and CO are held to mean values measured at the ground site during this spin-up period. In addition, we fix methane at a mixing ratio of 1.8 ppmv. Over the entirety of a model run temperature is held constant at 25 °C and the aerosol surface area concentration is held constant at 350 $\mu m^2 cm^{-3}$, which represents some of the largest aerosol surface are concentrations encountered by the R/V *Atlantis* while sampling Los Angeles outflow. The box model does not attempt to replicate the effects of meteorology and thus the processes of dilution and deposition are not accurately incorporated.

To maintain reasonable concentrations of the many modeled species which were not constrained by observations, we apply a continuous dilution rate of 1.5 % h^{-1} to all species. Formaldehyde and nitric acid have an additional deposition rate of 30 % h^{-1} in order to keep mixing ratios at levels most similar to those sampled during the CalNex study (< 6 ppbv for formaldehyde) (Warneke et al., 2011). The sensitivity of the results to this additional loss rate is minor (< 20 % adjustments to the Cl· budget), and the need for this additional loss is likely related to our neglect of deposition for intermediate organic oxidation products (in the case of formaldehyde) and of HNO_3 itself. Isoprene, alpha-pinene, beta-pinene, and limonene are allowed to freely evolve at night during the spin-up period to avoid unrealistic conditions whereby NO_3 reactions with these compounds proceeded indefinitely throughout the night. That is, we assume that advection of air masses from the land out over the water (either at the surface or aloft of the continental nocturnal surface layer) would ultimately limit the source of reactive biogenic VOC. At hour 69, which represents sunset on the third model day, all species are released from observational constraints and the chemistry evolves freely for another 27 h. We use the final 24 h of a model run as the analysis period. All figures and calculations described here are performed on the model output from this period.

A number of reactions necessary for evaluating Cl· production and reactivity are not included in the MCM. Version 3.2 of the MCM only includes Cl· reactions with alkanes. In order to accurately represent the chemistry, multiple mechanisms were added to the model framework. These include the Reactions (R1)–(R3), (R8), (R13)–(R21), and a number of VOC + Cl· reactions such as those for methanol, ethanol, isopropanol, ethene, propene, formaldehyde, ethanal, propanal, acetone, benzene, styrene, o-xylene, toluene. Several of the added mechanisms are explicitly shown in the Supplement (Figs. S2–S6). The reaction rate constants and product branching for these reactions were taken from the IUPAC kinetics database. Chlorinated products not present in the MCM or available in the IUPAC database were assumed to react similarly and with similar rate constants to non-chlorinated species of the same structure already in the MCM. Additionally, our revised mechanism explicitly tracks gas-phase HCl formation that results from hydrogen atom abstraction reactions by Cl·. $ClNO_2$ photolysis frequencies were estimated by scaling measured NO_2 photolysis frequencies down by a factor of 30 (i.e., $j_{NO_2}/30$). This approximation produces $ClNO_2$ photolysis frequencies close to observations taken aboard the R/V *Atlantis* (Fig. S7). Photolysis frequencies for $ClONO_2$ and HOCl were calculated using the Tropospheric Ultraviolet and Visible (TUV) Radiation Model (available at http://cprm.acd.ucar.edu/Models/TUV) and incorporated into the box model.

$$Cl\cdot + O_3 \rightarrow ClO + O_2 \tag{R13}$$

$$ClO + NO_2 \rightarrow ClONO_2 \tag{R14}$$

$$ClO + HO_2 \rightarrow HOCl + O_2 \tag{R15}$$

$$ClONO_2 + h\nu \rightarrow Cl\cdot + NO_3 \tag{R16}$$

$$ClONO_2 + h\nu \rightarrow ClO + NO_2 \tag{R17}$$

$$HOCl + h\nu \rightarrow Cl\cdot + OH \tag{R18}$$

$$ClONO_2 + H^+ + Cl^- \xrightarrow{\gamma} Cl_2 + HNO_3 \tag{R19}$$

$$HOCl + H^+ + Cl^- \xrightarrow{\gamma} Cl_2 + H_2O \tag{R20}$$

$$ClO + NO \rightarrow Cl\cdot + NO_2 \tag{R21}$$

For alkenes, the major pathway involves addition of chlorine to the double bond rather than the typical hydrogen abstraction pathway (Atkinson et al., 2004). This pathway leads to chlorinated products which might be detectable as tracers of Cl· chemistry in future studies. As we show below, such compounds could be another avenue for Cl· recycling. Reactions of Cl· with isoprene, which also produces unique chlorinated products, were not included in the model framework given its modest < 1 % contribution to total Cl· reactivity in the modeled Los Angeles outflow and the large increase in complexity when incorporating the mechanism (Fan and Zhang, 2004; Tanaka et al., 2003). Instead, the products of Cl· + isoprene were tracked as a single generic species with no chemical losses. However, in areas where isoprene is a more significant contributor to Cl· reactivity, it would be necessary to include a more explicit isoprene oxidation

mechanism to accurately capture the effects Cl·, especially to assess any chlorinated products that might form from these reactions (Riemer et al., 2008). In such locations the products of chlorine-initiated isoprene oxidation are likely more pronounced than in the Los Angeles region.

Gas-particle reaction probabilities in the model are set to 0.01 for N_2O_5, $ClONO_2$, and HOCl (R8, R19, R20). A $\gamma = 0.01$ is within the typical range of $\gamma(N_2O_5)$ measured on ambient aerosol (< 0.001–0.03) at elevated RH during various field studies (Bertram et al., 2009; Riedel et al., 2012b). Laboratory measurements of $ClONO_2$ and HOCl uptake under stratospheric and tropospheric conditions on sulfuric acid, sodium chloride, and sodium bromide particles and pure water droplets generally report γ values < 0.06 for $ClONO_2$ and HOCl (Deiber et al., 2004; Hanson and Ravishankara, 1994; Hanson et al., 1994). We make the upper-limit assumption that reactions of $ClONO_2$ and HOCl on aerosol particles produce only Cl_2 with unit efficiency. Given that Cl_2 production from heterogeneous reactions of $ClONO_2$ and HOCl is proportional to the product of γ and the yield, we use $\gamma = 0.01$ and a 100 % yield on all particles in the model.

To examine the effects of $ClNO_2$ formation, we vary φ_{ClNO_2} between 0 % and 50 % in successive model runs, which produce a without-$ClNO_2$ case and a with-$ClNO_2$ case, respectively. A 50 % yield results in ~ 1.5 ppbv of $ClNO_2$ as shown in Fig. 1, which is similar to levels in the Los Angeles outflow conditions encountered during CalNex. We also performed a series of model runs where HONO was constrained to observations made at the Pasadena ground site. Its abundance otherwise is determined only by the reaction of OH + NO, HONO + OH, and the photolysis of HONO. Most of our main conclusions reported here are relatively insensitive to HONO. Moreover, the vertical profiles of $ClNO_2$ and HONO throughout the nocturnal and evolving daytime boundary layer are likely different (Young et al., 2012), making our primary focus on $ClNO_2$ a reasonable simplification for a box model.

3 Results and discussion

3.1 Cl-atom budget

The model predicts that, integrated over a typical day in the Los Angeles outflow, $ClNO_2$ is the major driver of Cl· evolution. Neither HCl + OH nor multiphase chemistry involving $ClONO_2$ and HOCl to produce Cl_2 are competitive with the $ClNO_2$ source. Moreover, this picture is consistent with that derived solely from observations in this region (Riedel et al., 2012a). Figure 1 shows the Cl· concentration predicted by the model during the 24 h analysis period for both the with-$ClNO_2$ and without-$ClNO_2$ cases. When $ClNO_2$ formation is included, the Cl· concentration reaches a maximum at ~ 7 a.m. (2 h after model sunrise) with a value of 1.08×10^5 atoms cm^{-3}. A substantially different picture results from the without-$ClNO_2$ case where the maximum Cl· concentration occurs around noon and only reaches 0.2×10^5 atoms cm^{-3}. The assumptions made about the aerosol reaction probabilities of $ClONO_2$ and HOCl partially drive the late afternoon Cl· profile, which, as a result, is more uncertain. However, this afternoon Cl· concentration profile is not especially sensitive to the assumed reaction probabilities. For example, increasing the reaction probabilities of $ClONO_2$ and HOCl from 0.01 to 0.1 does not substantially change the 24 h profile. The maximum in Cl· concentration is increased by ~ 10 % still occurring in the early morning hours after sunrise (~ 7 a.m.), and the integrated Cl· concentration over the entire day is enhanced by only 20 %. Additionally, the choice of 0.01 for a $ClONO_2$ and HOCl reaction probability and a 100 % Cl_2 yield is likely more realistic as the formation of Cl_2 from these reactions is unlikely to be the sole product (Caloz et al., 1996; Santschi and Rossi, 2005). That said, to fully understand the impact of Cl· chemistry in coastal urban areas, the fate of $ClONO_2$ especially needs to be better constrained.

The evolution of Cl· largely follows that of the dominant source terms, as shown in Fig. 2. In the absence of $ClNO_2$ formation (Fig. 2a), the bulk of Cl· production results from the HCl + OH production channel, and the maximum in Cl· production rate of

0.5×10^6 atoms cm^{-3} s^{-1} coincides with the maximum production from the HCl + OH channel. In the with-$ClNO_2$ case (Fig. 2b), the maximum Cl· production rate occurs at 7 a.m. with a value of 3.4×10^6 atoms cm^{-3} s^{-1} corresponding to the maximum contribution from $ClNO_2$ photolysis. The $ClNO_2$ production channel represents 56 % of Cl· production over the course of the entire day, leading to nearly 3.7 times as many Cl· produced relative to the without-$ClNO_2$ case. By noon, $ClNO_2$ is largely depleted under the clear-sky model conditions, and other Cl· production channels like the reaction of HCl with OH and the photolysis of Cl_2 from HOCl and $ClONO_2$ heterogeneous chemistry become more dominant. These production channels involving multi-phase Cl-recycling to form Cl_2 show significant enhancements when $ClNO_2$ formation is included. For example, Cl· production from $ClONO_2$ photolysis, HOCl photolysis, and Cl_2 photolysis are enhanced by factors of 3.3, 2.2, and 3.3, respectively over the without-$ClNO_2$ case. To some extent these enhancements should be expected considering the larger Cl· pool available for recycling reactions when $ClNO_2$ formation is allowed, but they give indication of the degree of indirect coupling between $ClNO_2$ and Cl_2 via the increased formation of reactive chlorine reservoirs like $ClONO_2$ and HOCl. During CalNex, molecular chlorine was also measured along with $ClNO_2$ (Riedel et al., 2012a). Observations of nighttime and early morning Cl_2 were typically in the 5–50 pptv range. Modeled Cl_2 levels are of similar magnitude to these observations, as well as previous observations of Cl_2 in this region (Finley and Saltzman, 2006, 2008), and show a morning enhancement with slightly elevated levels throughout the day but only with the inclusion of $ClNO_2$ (see Fig. S8).

Given the lack of BrCl observations outside of polar regions, we do not include BrCl formation in the model and therefore do not explicitly account for the potential Cl· source, if any, represented by BrCl. Considering Cl_2 represents 16 % of the integrated Cl· source over the course of a model day, the typical seawater ratio of chloride to bromide of ~ 650 : 1, and assuming that BrCl formation is not significantly faster than 650 times Cl_2 formation, we estimate an upper limit Cl· source from BrCl resulting from $ClONO_2$ and HOCl reactions that is similar to that predicted from Cl_2. That said, BrCl

Discussion Paper | Discussion Paper | Discussion Paper | Discussion Paper |

formed from these reactions should not significantly bias our Cl· estimates considering that we force these reactants to produce exclusively Cl_2, the photolysis of which forms 2Cl· compared to only 1Cl· from BrCl photolysis. However, heterogeneous reactions of $BrONO_2$ and HOBr to form BrCl are not accounted for at all. Using maximum HCl levels as a measure of particulate chloride displaced over Los Angeles and the expected chloride to bromide ratio in seawater, 2.5 ppbv of chloride corresponds to ~ 4 pptv of bromide available for BrCl formation. Incorporating this amount of total bromine into the model and assuming $\gamma(BrONO_2)$ and $\gamma(HOBr) = 0.1$ with a unit yield of BrCl, we predict the model could be neglecting a Cl· source from BrCl on the order of 5 % of the Cl· concentration integrated over the model day. Ambient measurements of BrCl in polluted coastal regions would be a particularly useful constraint on the extent of these Cl· recycling reactions and the role of bromide.

The use of a comprehensive chemical mechanism such as the MCM also illustrates a potentially important but heretofore overlooked source of Cl· in polluted regions. In the with-$ClNO_2$ case, the reaction of OH with formyl chloride (CHOCl), produced from Cl· attack of alkenes, becomes a noticeable Cl· source during the afternoon. Interestingly, CHOCl photolysis is predicted to be a Cl· source comparable in magnitude to that from HOCl photolysis (Fig. 2b). In fact, because we possibly overestimate the actual multiphase recycling of $ClONO_2$ and HOCl to form Cl_2, Cl· release from such acid chlorides may be more important than these multiphase processes in regions with significant alkene concentrations. This result suggests observations of acid chlorides would be as beneficial as Cl_2 in polluted regions.

HONO has a noticeable impact on the afternoon Cl· budget via photolysis to form OH followed by the reaction of OH + HCl. Constraining the model to the HONO diurnal profile measured at the Pasadena ground site leads to a 60 % increase (1.4×10^7 to 2.26×10^7 molecules cm^{-3}) in the daily maximum OH concentration and a similar increase in the integrated Cl· formation rate from OH + HCl. Multiphase recycling via $ClONO_2$ and HOCl are also increased as a result of the larger Cl· concentrations. However, as discussed by Young et al. (2012), afternoon and daytime HONO concentrations

are fairly uncertain, especially when considering the extent to which HONO measurements over land represent HONO concentrations in the marine boundary layer during morning hours within an air mass that was transported offshore overnight.

We also investigate the formation potential of chlorinated products at potentially detectable quantities resulting from the Cl· oxidation of VOC. These species could represent "tracers" of Cl· chemistry and indicate the extent to which Cl· oxidation reactions are occurring. This issue has been investigated previously in the Houston area using ground based measurements of potential products from Cl· oxidation of isoprene (Riemer et al., 2008). As stated above, chlorinated products of Cl· reactions with isoprene are not included our model and are likely of minor importance to total Cl· reactivity in the Los Angeles region. Within our model framework, Cl· addition reactions with ethene and propene can produce chlorinated products such as 2-chloroperoxypropionyl nitrate (2-chloroPPN), chloroacetaldehyde, 2-chloroperoxyacetyl nitrate (2-chloroPAN), formyl chloride, 2-chloropropanal, and chloroacetone – some of which have been previously investigated in polar regions (Keil and Shepson, 2006). As with most of the previously mentioned effects, these enhancements are pronounced in the early part of the day when Cl· and VOC concentrations are highest in the model. As we show in Fig. 3, morning enhancements are typically on the order of 5–30 pptv above the background generated during the spin-up period. Chloroacetaldehyde and formyl chloride exhibit the largest enhancements.

In a polluted region such as the Los Angeles basin and outflow, Cl· will be primarily lost through reactions with VOC. Cl· reactivity as determined by the model is illustrated in Fig. 4, where it is broken into Cl· reactions with methane, alkanes, alkenes, alcohols, carbonyls (aldehydes and ketones), and ozone. Other Cl· + VOC reactions, such as reactions with aromatics, are not shown as they were not a significant sink of Cl· relative to the species listed. In the morning (7 a.m.), the bulk of reactivity is due to reactions with a variety of alkanes, which comprise 42 % of the 44 s^{-1} total reactivity. Later in the day (3 p.m.), as the VOC are consumed in the model and O_3 maximizes, the reaction with O_3 to form ClO is the dominant Cl· sink and represents about 60 % of the 39 s^{-1}

total reactivity. However, the majority of ClO (77 % at 7 a.m. and 67 % at 3 p.m.) will react with NO to give NO_2 and reform Cl· that can terminally react with VOC. Thus, we predict only 23–33 % of the Cl· + O_3 reactions produce stable reservoirs like $ClONO_2$ and HOCl; though other studies predict even less for the Los Angeles region (Young et al., 2013). Over the course of the day, no single VOC dominates the Cl· reactivity (see Fig. S9). Methane is consistently about 10 % of the total. This implies that all VOC reactive towards Cl· are relevant when trying to estimate the total reactivity and that only using a small subset may significantly underestimate the total. This behavior is different from that of OH, the reactivity of which is often dominated by a few VOC or inorganic species such as CO and NO_2 in highly polluted regions (Kato et al., 2011; Ren et al., 2003).

3.2 Impact on RO_x and NO_x

The $ClNO_2$ formation described above leads to important and unique impacts on processes relevant to tropospheric air quality. Cl· produced by $ClNO_2$ photolysis will react with VOC to produce RO_2 during morning hours. The RO_2 will primarily react with NO under the polluted conditions to form HO_2 and closed-shell oxygenated VOC or an alkyl nitrate. Alternatively, given the large NO_2/NO ratio during the morning, enhanced peroxy nitrate formation is possible via reaction of acyl peroxy radicals with NO_2. The HO_2 produced via RO_2 + NO also reacts with NO to form OH, which in turn reacts with VOC to form RO_2. The chain length of this cycle tends to be somewhat short in the morning given higher concentrations of NO_x leading to termination via OH + NO_2 to form HNO_3 which is efficiently removed from the atmosphere through wet and dry deposition. Nonetheless, Cl· will enhance the abundance of morning time RO_x (OH + HO_2 + RO_2) as illustrated in Fig. 5 which will lead to enhanced O_3 production rates relative to a model run without $ClNO_2$.

Figure 5a shows the HO_x production rate (P_{HO_x}) for both the with- and without-$ClNO_2$ cases. A factor of 2.2 increase occurs in the early morning hours around 7 a.m. when Cl· production from $ClNO_2$ photolysis is the major Cl· source. P_{HO_x} remains elevated

throughout the day relative to the without-$ClNO_2$ case likely due to the larger ozone values in the with-$ClNO_2$ case, thus illustrating that the $ClNO_2$ influence persists for more than just the early morning hours. 24 h integrated HO_x production for the with- and without-$ClNO_2$ cases is 75 ppbv and 62 ppbv, respectively. Uncertainties in modeling HONO have the largest impact on quantifying the perturbation of $ClNO_2$ to P_{HO_x}. Constraining modeled HONO to the diel average values measured at the ground site results in the same overall pattern of $ClNO_2$ effects on P_{HO_x} described above, just at a reduced relative magnitude – i.e., the inclusion of $ClNO_2$ formation increases P_{HO_x} by ~ 35 % in the morning, with moderate enhancements to P_{HO_x} sustained throughout the day resulting in an integrated P_{HO_x} of 116 ppbv and 105 ppbv for the with- and without $ClNO_2$ cases, respectively. These two extremes in terms of HONO are likely both representative – the latter HONO-rich case being representative of near surface chemistry while the former HONO-poor case is more representative of the residual boundary layer aloft of the surface, which dominants the column-average radical budget as described by Young et al. (2012).

Figure 5b shows the effects of $ClNO_2$ on OH, HO_2, the sum over all 717 organic peroxy radicals (RO_2), and the sum of 140 acyl peroxy nitrates (APN) predicted by the model. The ratio of the with-$ClNO_2$ case relative to the without-$ClNO_2$ case is shown. Inclusion of $ClNO_2$ formation results in significant changes in HO_x (OH and HO_2) with 190 % and 220 % enhancements during the morning hours in OH and both HO_2 and RO_2, respectively. Such enhancements could be partly related to noted discrepancies between measured and modeled morning HO_x levels (Dusanter et al., 2009; Mao et al., 2010; Ren et al., 2003). Comparable enhancements in HO_2 and RO_2 were predicted by Osthoff et al. (2008) using the MCM to assess measurements taken in and around the Houston ship channel. In remote low-NO_x regions, Cl· and OH are largely uncoupled such that the presence of one does not largely impact the abundance of the other. This condition then allows indirect quantification of Cl· abundance by comparing VOC which have different reaction rate constants for reaction with OH and Cl· (i.e., Jobson et al. (1994), Platt et al. (2004), and Allan et al., 2007). However, the presence of ad-

Discussion Paper | Discussion Paper | Discussion Paper | Discussion Paper |

ditional Cl· from $ClNO_2$ in a polluted region has the potential to significantly increase OH via the above mechanism, especially in the morning hours thereby muting this effect. Constraining modeled HONO again lowers the magnitude of these $ClNO_2$ induced morning perturbations to 25 and 50 % increases in OH and the sum of HO_2 and RO_2, respectively. Again, while even these HONO-rich perturbations are significant, these findings, together with the vertically resolved estimates of Young et al. (2012), further imply that strong vertical gradients in HONO will influence the $ClNO_2$ effects on morning oxidant evolution.

$ClNO_2$ formation and photolysis has implications for the reactive nitrogen budget as well. $ClNO_2$ is relatively unreactive at night in these regions, thereby building up and allowing transport of NO_x downwind of the urban core with morning photolysis of $ClNO_2$ analogous to thermal decomposition of acyl peroxy nitrates such as PAN. In addition to this direct impact on NO_x transport, we find significant perturbations to acyl peroxy nitrate formation to occur in the with-$ClNO_2$ case (see Fig. 5b). A 50 % enhancement in total APN occurs before noon, and the enhancement remains elevated at around 10 % for the remainder of the day. This $ClNO_2$ induced perturbation to APN formation largely persists even when measured HONO values are incorporated. Additionally, the sum of alkyl nitrates is also enhanced by 15 % before noon with individual alkyl nitrates enhanced up to 60 % in the with-$ClNO_2$ case. Increasing the partitioning of NO_x into reservoirs such as APN implies a greater potential for export of NO_x to remote regions. In fact, while $ClNO_2$ formation extends the lifetime of NO_x through the night, our model suggests that faster OH + NO_2, APN formation, and alkyl nitrate formation due to increased RO_x levels during the subsequent day largely offset this effect, such that NO_x is ~ 6 % lower from sunrise until noon in the with-$ClNO_2$ than in the without-$ClNO_2$ case.

3.3 Impact on ozone production rate and odd-oxygen

We illustrate the influence of $ClNO_2$ chemistry on ozone production in Fig. 5c. Over the entire model day, the difference between the integrated ozone production rate

with 1.5 ppbv $ClNO_2$ and the integrated ozone production rate without $ClNO_2$ is about 12 ppbv. The majority of this enhancement takes place over the first 5 h after sunrise where at 6.30 a.m. the ozone production rate is enhanced by ~ 200 %. The pre-noon ozone mixing ratios relative to the without-$ClNO_2$ case are increased by ~ 20 % with ~ 10 % increase over the remainder of the day including peak ozone which occurs at about 5 p.m. Such an influence is potentially large enough to affect attainment of air quality standards in polluted coastal regions where exceedences are often only tens of ppbv over the current standard (Parrish et al., 2010; Qin et al., 2004; US EPA, 2006). The enhancement in ozone production scales nearly linearly with the $ClNO_2$ yield for this region, as expected, given that the ozone production rate is approximately linear with the primary radical source in a NO_x-saturated environment like Los Angeles. Constraining modeled HONO to the observations results in a slightly smaller 9 ppbv enhancement in the integrated ozone production rate due to $ClNO_2$ chemistry.

The above result is also interesting to consider in terms of the impact of nocturnal nitrogen oxide chemistry on the odd-oxygen budget. Defining O_x as the sum of O_3 and NO_2, our model predicts that N_2O_5 reactions on aerosol particles consume 9 ppbv O_x at night. If we neglect $ClNO_2$ formation, this 9 ppbv O_x is permanently lost due to nitrate formation from N_2O_5 hydrolysis. However, incorporating $ClNO_2$ formation, with a yield (branching ratio) of 50 %, results in up to 12 ppbv O_x produced the subsequent day compared to the case where $ClNO_2$ formation is neglected. Thus, due to $ClNO_2$ formation and its daytime impact on oxidants and ozone, nighttime N_2O_5 chemistry does not net destroy O_x but is in fact potentially a net source, or at least a null cycle, for the Los Angeles region conditions we simulate here.

While not directly comparable, our results appear generally consistent with a recent 3-D CMAQ modeling study of $ClNO_2$ effects on ozone and particulate nitrate (Sarwar et al., 2012). In the Los Angeles region, the CMAQ modeling showed roughly a 2–4 ppbv increase in daytime ozone per ppbv $ClNO_2$ photolyzed, with maxima approaching 8 ppbv ppbv^{-1}. Likely important in setting the actual ozone enhancement caused by $ClNO_2$ is, among other possibilities, the extent to which a model mixes background marine air with the polluted core during transport and the model predicted vertical distribution of $ClNO_2$. These issues will be important to test with observations in order to validate model representations of this process.

4 Summary and conclusions

These model results suggest that $ClNO_2$ photolysis is likely a major Cl· source, if not the dominant source, under conditions similar to those sampled in the Los Angeles region during CalNex 2010. The impact of $ClNO_2$ on potential daytime halogen atom recycling is substantial, with significant enhancements predicted on other Cl· reservoirs like $ClONO_2$, HOCl, and Cl_2. Relative to model runs without $ClNO_2$ formation, the presence of $ClNO_2$ causes significant and non-negligible perturbations in HO_x, RO_2, APN, and ozone production. Relative to a model without $ClNO_2$ formation and heterogeneous HONO production, incorporating $ClNO_2$ perturbed the integrated total radical and ozone production rates by 20 %, with perturbations in RO_x and APN > 100 %. Moreover, we show that, given these effects, the impact of N_2O_5 reactions on aerosol particles is not a net sink of odd-oxygen but instead a net source for the polluted coastal conditions we model here. The absolute magnitude of the perturbations in these quantities and processes relative to a model that does not include $ClNO_2$ will ultimately depend upon the presence of HONO and the abundance of $ClNO_2$ and HONO vertically as well as seasonally.

We conclude by noting that during winter, in locations such as the northeastern US, the role of $ClNO_2$ may be substantially more important to the total radical budget given that $O(^1D)$ production and H_2O vapor concentrations can both be factors of 5 lower than presented here, resulting in more than an order of magnitude reduction in primary OH abundances while $ClNO_2$ approaches similar concentrations (Kercher et al., 2009). This idea is consistent with the apparently important role of $ClNO_2$ at inland locations during wintertime as illustrated by recent studies at the Uintah Basin, Utah (Edwards et al., 2013).

Supplementary material related to this article is available online at http://www.atmos-chem-phys-discuss.net/13/28973/2013/acpd-13-28973-2013-supplement.pdf.

Acknowledgements. This work was supported by a grant from the National Science Foundation (NSF CAREER ATM-0846183 to J. A. Thornton). T. P. Riedel is grateful for an Earth System Science graduate fellowship from the National Aeronautics and Space Administration (NASA NESSF NNX10AN48H). G. M. Wolfe acknowledges support from a NOAA Climate and Global Change Postdoctoral Fellowship administered by the University Corporation for Atmospheric Research. This research was support in part by the NOAA Health of the Atmosphere Program. We also thank the crew of the R/V *Atlantis* and the Pasadena ground site science team for their tireless efforts and continual support throughout the CalNex study.

References

Allan, W., Struthers, H., and Lowe, D. C.: Methane carbon isotope effects caused by atomic chlorine in the marine boundary layer: global model results compared with Southern Hemisphere measurements, J. Geophys. Res.-Atmos., 112, D04306, doi:10.1029/2006jd007369, 2007.

Atkinson, R., Baulch, D. L., Cox, R. A., Crowley, J. N., Hampson, R. F., Hynes, R. G., Jenkin, M. E., Rossi, M. J., and Troe, J.: Evaluated kinetic and photochemical data for atmospheric chemistry: Volume I - gas phase reactions of O_x, HO_x, NO_x and SO_x species, Atmos. Chem. Phys., 4, 1461–1738, doi:10.5194/acp-4-1461-2004, 2004.

Badger, C. L., Griffiths, P. T., George, I., Abbatt, J. P. D., and Cox, R. A.: Reactive uptake of N_2O_5 by aerosol particles containing mixtures of humic acid and ammonium sulfate, J. Phys. Chem. A, 110, 6986–6994, doi:10.1021/jp0562678, 2006.

Bertram, T. H. and Thornton, J. A.: Toward a general parameterization of N_2O_5 reactivity on aqueous particles: the competing effects of particle liquid water, nitrate and chloride, Atmos. Chem. Phys., 9, 8351–8363, doi:10.5194/acp-9-8351-2009, 2009.

Bertram, T. H., Thornton, J. A., Riedel, T. P., Middlebrook, A. M., Bahreini, R., Bates, T. S., Quinn, P. K., and Coffman, D. J.: Direct observations of N_2O_5 reactivity on ambient aerosol particles, Geophys. Res. Lett., 36, L19803, doi:10.1029/2009gl040248, 2009.
Bloss, C., Wagner, V., Jenkin, M. E., Volkamer, R., Bloss, W. J., Lee, J. D., Heard, D. E., Wirtz, K., Martin-Reviejo, M., Rea, G., Wenger, J. C., and Pilling, M. J.: Development of a detailed chemical mechanism (MCMv3.1) for the atmospheric oxidation of aromatic hydrocarbons, Atmos. Chem. Phys., 5, 641–664, doi:10.5194/acp-5-641-2005, 2005.
Buys, Z., Brough, N., Huey, L. G., Tanner, D. J., von Glasow, R., and Jones, A. E.: High temporal resolution Br_2, BrCl and BrO observations in coastal Antarctica, Atmos. Chem. Phys., 13, 1329–1343, doi:10.5194/acp-13-1329-2013, 2013.
Caloz, F., Fenter, F. F., and Rossi, M. J.: Heterogeneous kinetics of the uptake of $ClONO_2$ on NaCl and KBr, J. Phys. Chem., 100, 7494–7501, doi:10.1021/jp953099i, 1996.
Daum, P. H., Kleinman, L., Imre, D. G., Nunnermacker, L. J., Lee, Y. N., Springston, S. R., Newman, L., and Weinstein-Lloyd, J.: Analysis of the processing of Nashville urban emissions on 3 July and 18 July 1995, J. Geophys. Res.-Atmos., 105, 9155–9164, doi:10.1029/1999jd900997, 2000.
Deiber, G., George, Ch., Le Calvé, S., Schweitzer, F., and Mirabel, Ph.: Uptake study of $ClONO_2$ and $BrONO_2$ by Halide containing droplets, Atmos. Chem. Phys., 4, 1291–1299, doi:10.5194/acp-4-1291-2004, 2004.
Dusanter, S., Vimal, D., Stevens, P. S., Volkamer, R., Molina, L. T., Baker, A., Meinardi, S., Blake, D., Sheehy, P., Merten, A., Zhang, R., Zheng, J., Fortner, E. C., Junkermann, W., Dubey, M., Rahn, T., Eichinger, B., Lewandowski, P., Prueger, J., and Holder, H.: Measurements of OH and HO_2 concentrations during the MCMA-2006 field campaign – Part 2: Model comparison and radical budget, Atmos. Chem. Phys., 9, 6655–6675, doi:10.5194/acp-9-6655-2009, 2009.
Edwards, P. M., Young, C. J., Aikin, K., deGouw, J., Dubé, W. P., Geiger, F., Gilman, J., Helmig, D., Holloway, J. S., Kercher, J., Lerner, B., Martin, R., McLaren, R., Parrish, D. D., Peischl, J., Roberts, J. M., Ryerson, T. B., Thornton, J., Warneke, C., Williams, E. J., and Brown, S. S.: Ozone photochemistry in an oil and natural gas extraction region during winter: simulations of a snow-free season in the Uintah Basin, Utah, Atmos. Chem. Phys., 13, 8955–8971, doi:10.5194/acp-13-8955-2013, 2013.
Fan, J. and Zhang, R.: Atmospheric oxidation mechanism of isoprene, Environ. Chem., 1, 140–149, doi:10.1071/en04045, 2004.

Finlayson-Pitts, B. J., Ezell, M. J., and Pitts, J. N.: Formation of chemically active chlorine compounds by reactions of atmospheric NaCl particles with gaseous N_2O_5 and $ClONO_2$, Nature, 337, 241–244, doi:10.1038/337241a0, 1989.
Finley, B. D. and Saltzman, E. S.: Measurement of Cl_2 in coastal urban air, Geophys. Res. Lett., 33, L11809, doi:10.1029/2006gl025799, 2006.
Finley, B. D. and Saltzman, E. S.: Observations of Cl_2, Br_2, and I_2 in coastal marine air, J. Geophys. Res.-Atmos., 113, D21301, doi:10.1029/2008jd010269, 2008.
Foster, K. L., Plastridge, R. A., Bottenheim, J. W., Shepson, P. B., Finlayson-Pitts, B. J., and Spicer, C. W.: The role of Br_2 and BrCl in surface ozone destruction at polar sunrise, Science, 291, 471–474, doi:10.1126/science.291.5503.471, 2001.
Hanson, D. R. and Ravishankara, A. R.: Reactive uptake of $ClONO_2$ onto sulfuric-acid due to reaction with HCl and H_2O, J. Phys. Chem., 98, 5728–5735, doi:10.1021/j100073a026, 1994.
Hanson, D. R., Ravishankara, A. R., and Solomon, S.: Heterogeneous reactions in sulfuric-acid aerosols – a framework for model-calculations, J. Geophys. Res.-Atmos., 99, 3615–3629, doi:10.1029/93jd02932, 1994.
Jaegle, L., Steinberger, L., Martin, R. V., and Chance, K.: Global partitioning of NO_x sources using satellite observations: relative roles of fossil fuel combustion, biomass burning and soil emissions, Faraday Discuss., 130, 407–423, doi:10.1039/B502128F, 2005.
Jenkin, M. E., Saunders, S. M., and Pilling, M. J.: The tropospheric degradation of volatile organic compounds: a protocol for mechanism development, Atmos. Environ., 31, 81–104, doi:10.1016/s1352-2310(96)00105-7, 1997.
Jenkin, M. E., Saunders, S. M., Wagner, V., and Pilling, M. J.: Protocol for the development of the Master Chemical Mechanism, MCM v3 (Part B): tropospheric degradation of aromatic volatile organic compounds, Atmos. Chem. Phys., 3, 181–193, doi:10.5194/acp-3-181-2003, 2003.
Jobson, B. T., Niki, H., Yokouchi, Y., Bottenheim, J., Hopper, F., and Leaitch, R.: Measurements of C2–C6 hydrocarbons during the Polar Sunrise1992 Experiment: evidence for Cl atom and Br atom chemistry, J. Geophys. Res.-Atmos., 99, 25355–25368, doi:10.1029/94JD01243, 1994.
Karlsson, R. S. and Ljungström, E. B.: Laboratory study of ClNO: hydrolysis, Environ. Sci. Technol., 30, 2008–2013, doi:10.1021/es950801f, 1996.

Kato, S., Sato, T., and Kajii, Y.: A method to estimate the contribution of unidentified VOCs to OH reactivity, Atmos. Environ., 45, 5531–5539, doi:10.1016/j.atmosenv.2011.05.074, 2011.

Keene, W. C., Stutz, J., Pszenny, A. A. P., Maben, J. R., Fischer, E. V., Smith, A. M., von Glasow, R., Pechtl, S., Sive, B. C., and Varner, R. K.: Inorganic chlorine and bromine in coastal New England air during summer, J. Geophys. Res.-Atmos., 112, D10S12, doi:10.1029/2006jd007689, 2007.

Keil, A. D. and Shepson, P. B.: Chlorine and bromine atom ratios in the springtime Arctic troposphere as determined from measurements of halogenated volatile organic compounds, J. Geophys. Res.-Atmos., 111, D17303, doi:10.1029/2006JD007119, 2006.

Kercher, J. P., Riedel, T. P., and Thornton, J. A.: Chlorine activation by N_2O_5: simultaneous, in situ detection of $ClNO_2$ and N_2O_5 by chemical ionization mass spectrometry, Atmos. Meas. Tech., 2, 193–204, doi:10.5194/amt-2-193-2009, 2009.

Kleinman, L. I.: The dependence of tropospheric ozone production rate on ozone precursors, Atmos. Environ., 39, 575–586, doi:10.1016/j.atmosenv.2004.08.047, 2005.

Lawler, M. J., Sander, R., Carpenter, L. J., Lee, J. D., von Glasow, R., Sommariva, R., and Saltzman, E. S.: HOCl and Cl_2 observations in marine air, Atmos. Chem. Phys., 11, 7617–7628, doi:10.5194/acp-11-7617-2011, 2011.

Mao, J., Ren, X., Chen, S., Brune, W. H., Chen, Z., Martinez, M., Harder, H., Lefer, B., Rappenglück, B., Flynn, J., and Leuchner, M.: Atmospheric oxidation capacity in the summer of Houston 2006: comparison with summer measurements in other metropolitan studies, Atmos. Environ., 44, 4107–4115, doi:10.1016/j.atmosenv.2009.01.013, 2010.

McNeill, V. F., Patterson, J., Wolfe, G. M., and Thornton, J. A.: The effect of varying levels of surfactant on the reactive uptake of N_2O_5 to aqueous aerosol, Atmos. Chem. Phys., 6, 1635–1644, doi:10.5194/acp-6-1635-2006, 2006.

Mentel, T. F., Sohn, M., and Wahner, A.: Nitrate effect in the heterogeneous hydrolysis of dinitrogen pentoxide on aqueous aerosols, Phys. Chem. Chem. Phys., 1, 5451–5457, doi:10.1039/a905338g, 1999.

Mielke, L. H., Furgeson, A., and Osthoff, H. D.: Observation of $ClNO_2$ in a mid-continental urban environment, Environ. Sci. Technol., 45, 8889–8896, doi:10.1021/es201955u, 2011.

Osthoff, H. D., Roberts, J. M., Ravishankara, A. R., Williams, E. J., Lerner, B. M., Sommariva, R., Bates, T. S., Coffman, D., Quinn, P. K., Dibb, J. E., Stark, H., Burkholder, J. B., Talukdar, R. K., Meagher, J., Fehsenfeld, F. C., and Brown, S. S.: High levels of nit-

ryl chloride in the polluted subtropical marine boundary layer, Nat. Geosci., 1, 324–328, doi:10.1038/ngeo177, 2008.

Parrish, D. D., Aikin, K. C., Oltmans, S. J., Johnson, B. J., Ives, M., and Sweeny, C.: Impact of transported background ozone inflow on summertime air quality in a California ozone exceedance area, Atmos. Chem. Phys., 10, 10093–10109, doi:10.5194/acp-10-10093-2010, 2010.

Phillips, G. J., Tang, M. J., Thieser, J., Brickwedde, B., Schuster, G., Bohn, B., Lelieveld, J., and Crowley, J. N.: Significant concentrations of nitryl chloride observed in rural continental Europe associated with the influence of sea salt chloride and anthropogenic emissions, Geophys. Res. Lett., 39, L10811, doi:10.1029/2012gl051912, 2012.

Platt, U., Allan, W., and Lowe, D.: Hemispheric average Cl atom concentration $^{13}C/^{12}C$ ratios in atmospheric methane, Atmos. Chem. Phys., 4, 2393–2399, doi:10.5194/acp-4-2393-2004, 2004.

Qin, Y., Tonnesen, G. S., and Wang, Z.: One-hour and eight-hour average ozone in the California South Coast air quality management district: trends in peak values and sensitivity to precursors, Atmos. Environ., 38, 2197–2207, doi:10.1016/j.atmosenv.2004.01.010, 2004.

Raff, J. D., Njegic, B., Chang, W. L., Gordon, M. S., Dabdub, D., Gerber, R. B., and Finlayson-Pitts, B. J.: Chlorine activation indoors and outdoors via surface-mediated reactions of nitrogen oxides with hydrogen chloride, P. Natl. Acad. Sci. USA, 106, 13647–13654, doi:10.1073/pnas.0904195106, 2009.

Ren, X. R., Harder, H., Martinez, M., Lesher, R. L., Oliger, A., Simpas, J. B., Brune, W. H., Schwab, J. J., Demerjian, K. L., He, Y., Zhou, X. L., and Gao, H. G.: OH and HO_2 chemistry in the urban atmosphere of New York City, Atmos. Environ., 37, 3639–3651, doi:10.1016/s1352-2310(03)00459-x, 2003.

Riedel, T. P., Bertram, T. H., Crisp, T. A., Williams, E. J., Lerner, B. M., Vlasenko, A., Li, S.-M., Gilman, J., de Gouw, J., Bon, D. M., Wagner, N. L., Brown, S. S., and Thornton, J. A.: Nitryl chloride and molecular chlorine in the coastal marine boundary layer, Environ. Sci. Technol., 46, 10463–10470, doi:10.1021/es204632r, 2012a.

Riedel, T. P., Bertram, T. H., Ryder, O. S., Liu, S., Day, D. A., Russell, L. M., Gaston, C. J., Prather, K. A., and Thornton, J. A.: Direct N_2O_5 reactivity measurements at a polluted coastal site, Atmos. Chem. Phys., 12, 2959–2968, doi:10.5194/acp-12-2959-2012, 2012b.

Riemer, D. D., Apel, E. C., Orlando, J. J., Tyndall, G. S., Brune, W. H., Williams, E. J., Lonneman, W. A., and Neece, J. D.: Unique isoprene oxidation products demonstrate chlorine

atom chemistry occurs in the Houston, Texas urban area, J. Atmos. Chem., 61, 227–242, doi:10.1007/s10874-009-9134-5, 2008.
Roberts, J. M., Osthoff, H. D., Brown, S. S., and Ravishankara, A. R.: N_2O_5 oxidizes chloride to Cl_2 in acidic atmospheric aerosol, Science, 321, 1059–1059, doi:10.1126/science.1158777, 2008.
Rubasinghege, G. and Grassian, V. H.: Surface-catalyzed chlorine and nitrogen activation: mechanisms for the heterogeneous formation of ClNO, NO, NO_2, HONO, and N_2O from HNO_3 and HCl on aluminum oxide particle surfaces, J. Phys. Chem. A, 116, 5180–5192, doi:10.1021/jp301488b, 2012.
Ryerson, T. B., Andrews, A. E., Angevine, W. M., Bates, T. S., Brock, C. A., Cairns, B., Cohen, R. C., Cooper, O. R., de Gouw, J. A., Fehsenfeld, F. C., Ferrare, R. A., Fischer, M. L., Flagan, R. C., Goldstein, A. H., Hair, J. W., Hardesty, R. M., Hostetler, C. A., Jimenez, J. L., Langford, A. O., McCauley, E., McKeen, S. A., Molina, L. T., Nenes, A., Oltmans, S. J., Parrish, D. D., Pederson, J. R., Pierce, R. B., Prather, K., Quinn, P. K., Seinfeld, J. H., Senff, C. J., Sorooshian, A., Stutz, J., Surratt, J. D., Trainer, M., Volkamer, R., Williams, E. J., and Wofsy, S. C.: The 2010 California research at the Nexus of air quality and climate change (CalNex) field study, J. Geophys. Res.-Atmos., 118, 5830–5866, doi:10.1002/jgrd.50331, 2013.
Santschi, C. and Rossi, M. J.: The heterogeneous interaction of HOCl with solid KBr substrates: the catalytic role of adsorbed halogens, Phys. Chem. Chem. Phys., 7, 2599–2609, doi:10.1039/b503071d, 2005.
Sarwar, G. and Bhave, P. V.: Modeling the effect of chlorine emissions on ozone levels over the eastern United States, J. Appl. Meteorol. Clim., 46, 1009–1019, doi:10.1175/jam2519.1, 2007.
Sarwar, G., Simon, H., Bhave, P., and Yarwood, G.: Examining the impact of heterogeneous nitryl chloride production on air quality across the United States, Atmos. Chem. Phys., 12, 6455–6473, doi:10.5194/acp-12-6455-2012, 2012.
Saunders, S. M., Jenkin, M. E., Derwent, R. G., and Pilling, M. J.: Protocol for the development of the Master Chemical Mechanism, MCM v3 (Part A): tropospheric degradation of non-aromatic volatile organic compounds, Atmos. Chem. Phys., 3, 161–180, doi:10.5194/acp-3-161-2003, 2003.

Scheer, V., Frenzel, A., Behnke, W., Zetzsch, C., Magi, L., George, C., and Mirabel, P.: Uptake of nitrosyl chloride (NOCl) by aqueous solutions, J. Phys. Chem. A, 101, 9359–9366, doi:10.1021/jp972143m, 1997.
Spicer, C. W., Chapman, E. G., Finlayson-Pitts, B. J., Plastridge, R. A., Hubbe, J. M., Fast, J. D., and Berkowitz, C. M.: Unexpectedly high concentrations of molecular chlorine in coastal air, Nature, 394, 353–356, doi:10.1038/28584, 1998.
Spicer, C. W., Plastridge, R. A., Foster, K. L., Finlayson-Pitts, B. J., Bottenheim, J. W., Grannas, A. M., and Shepson, P. B.: Molecular halogens before and during ozone depletion events in the Arctic at polar sunrise: concentrations and sources, Atmos. Environ., 36, 2721–2731, doi:10.1016/s1352-2310(02)00125-5, 2002.
Tanaka, P. L., Allen, D. T., McDonald-Buller, E. C., Chang, S., Kimura, Y., Mullins, C. B., Yarwood, G., and Neece, J. D.: Development of a chlorine mechanism for use in the carbon bond IV chemistry model, J. Geophys. Res.-Atmos., 108, 4145, doi:10.1029/2002jd002432, 2003.
Thornton, J. A., Braban, C. F., and Abbatt, J. P. D.: N_2O_5 hydrolysis on sub-micron organic aerosols: the effect of relative humidity, particle phase, and particle size, Phys. Chem. Chem. Phys., 5, 4593–4603, doi:10.1039/b307498f, 2003.
Thornton, J. A., Kercher, J. P., Riedel, T. P., Wagner, N. L., Cozic, J., Holloway, J. S., Dube, W. P., Wolfe, G. M., Quinn, P. K., Middlebrook, A. M., Alexander, B., and Brown, S. S.: A large atomic chlorine source inferred from mid-continental reactive nitrogen chemistry, Nature, 464, 271–274, doi:10.1038/nature08905, 2010.
US EPA: Air Quality Criteria for Ozone and Related Photochemical Oxidants (2006 Final), US Environmental Protection Agency, Washington, DC, EPA/600/R-05/004aF-cF, 2006.
Wagner, N. L., Riedel, T. P., Roberts, J. M., Thornton, J. A., Angevine, W. M., Williams, E. J., Lerner, B. M., Vlasenko, A., Li, S. M., Dube, W. P., Coffman, D. J., Bon, D. M., de Gouw, J. A., Kuster, W. C., Gilman, J. B., and Brown, S. S.: The sea breeze/land breeze circulation in Los Angeles and its influence on nitryl chloride production in this region, J. Geophys. Res.-Atmos., 117, D00V24, doi:10.1029/2012jd017810, 2012.
Warneke, C., Veres, P., Holloway, J. S., Stutz, J., Tsai, C., Alvarez, S., Rappenglueck, B., Fehsenfeld, F. C., Graus, M., Gilman, J. B., and de Gouw, J. A.: Airborne formaldehyde measurements using PTR-MS: calibration, humidity dependence, inter-comparison and initial results, Atmos. Meas. Tech., 4, 2345–2358, doi:10.5194/amt-4-2345-2011, 2011.

Wolfe, G. M. and Thornton, J. A.: The Chemistry of Atmosphere-Forest Exchange (CAFE) Model – Part 1: Model description and characterization, Atmos. Chem. Phys., 11, 77–101, doi:10.5194/acp-11-77-2011, 2011.

Young, C. J., Washenfelder, R. A., Roberts, J. M., Mielke, L. H., Osthoff, H. D., Tsai, C., Pikelnaya, O., Stutz, J., Veres, P. R., Cochran, A. K., VandenBoer, T. C., Flynn, J., Grossberg, N., Haman, C. L., Lefer, B., Stark, H., Graus, M., de Gouw, J., Gilman, J. B., Kuster, W. C., and Brown, S. S.: Vertically resolved measurements of nighttime radical reservoirs; in Los Angeles and their contribution to the urban radical budget, Environ. Sci. Technol., 46, 10965–10973, doi:10.1021/es302206a, 2012.

Young, C. J., Washenfelder, R. A., Edwards, P. M., Parrish, D. D., Gilman, J. B., Kuster, W. C., Mielke, L. H., Osthoff, H. D., Tsai, C., Pikelnaya, O., Stutz, J., Veres, P. R., Roberts, J. M., Griffith, S., Dusanter, S., Stevens, P. S., Flynn, J., Grossberg, N., Lefer, B., Holloway, J. S., Peischl, J., Ryerson, T. B., Atlas, E. L., Blake, D. R., and Brown, S. S.: Evaluating evidence for Cl sources and oxidation chemistry in a coastal, urban environment, Atmos. Chem. Phys. Discuss., 13, 13685–13720, doi:10.5194/acpd-13-13685-2013, 2013.

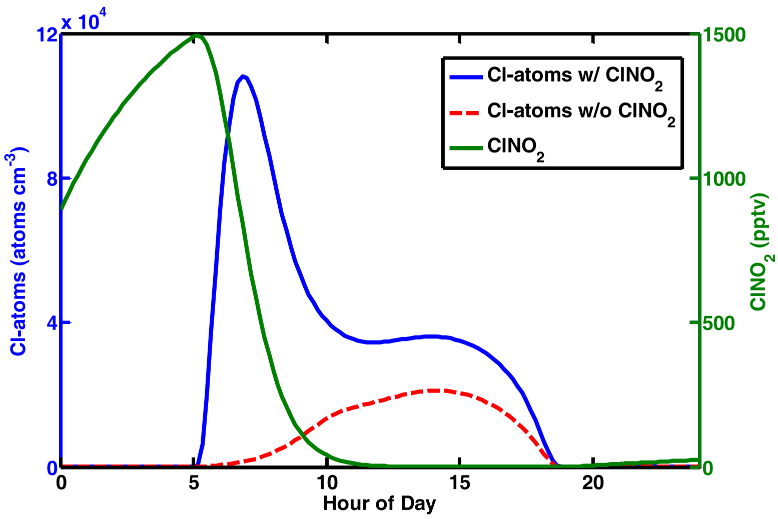

Fig. 1. Model output for the analysis period of a model run showing $ClNO_2$ mixing ratios (heavy green line, right *y* axis) and Cl· concentrations for the case including $ClNO_2$ formation (heavy blue line, left *y* axis) and the case excluding $ClNO_2$ formation (dashed red line, left *y* axis).

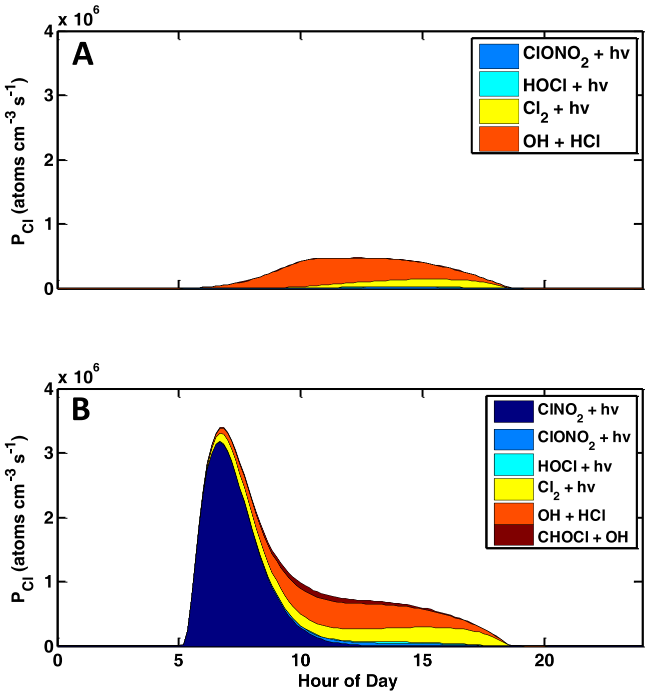

Fig. 2. Model calculated Cl· production channels **(A)** without $ClNO_2$ formation (top) and **(B)** with $ClNO_2$ formation (bottom).

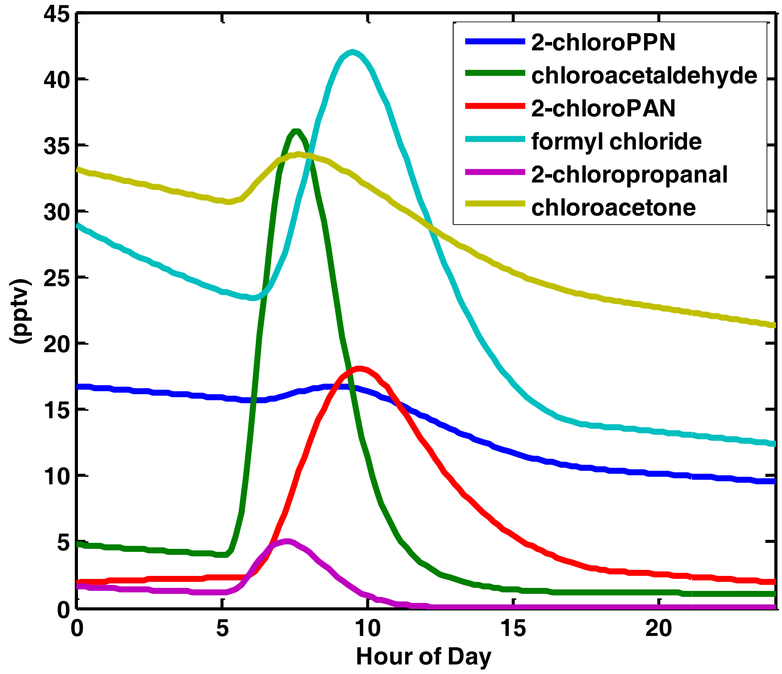

Fig. 3. Mixing ratios of various chlorinated species tracked in the model for the with-$ClNO_2$ model case.

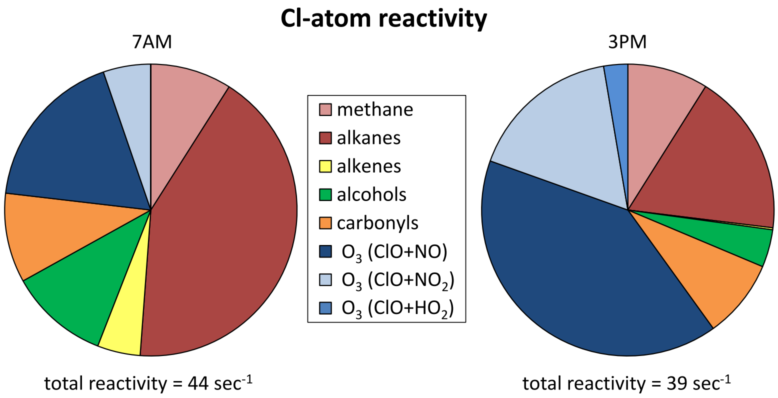

Fig. 4. Modeled Cl· reactivity at 7 a.m. (left) and 3 p.m. (right) grouped by reactant types.

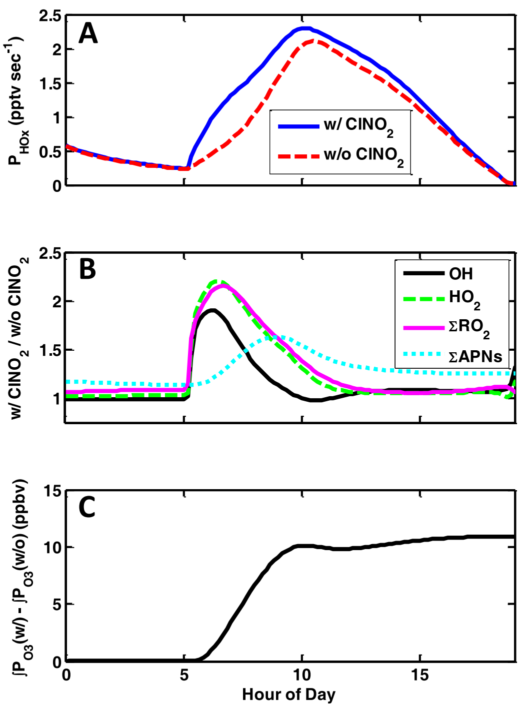

Fig. 5. (A) The HO_x production rate with $ClNO_2$ formation (solid blue line) and without $ClNO_2$ formation (dashed red line). **(B)** The ratio of the hydroxyl radical (solid black line), hydroperoxyl radical (dashed green line), sum of organic peroxy radicals (solid pink line), and sum of acyl peroxy nitrates (dotted cyan line) for the with-$ClNO_2$ case relative to the without-$ClNO_2$ case. **(C)** The difference between the integrated ozone production rate with $ClNO_2$ formation and the integrated ozone production rate without $ClNO_2$ formation.

Discussion Paper | Discussion Paper | Discussion Paper | Discussion Paper |